Polymer- and hybrid-based biomaterials for delivering biotherapeutic molecules in bone and cartilage tissue

García Couce, J.

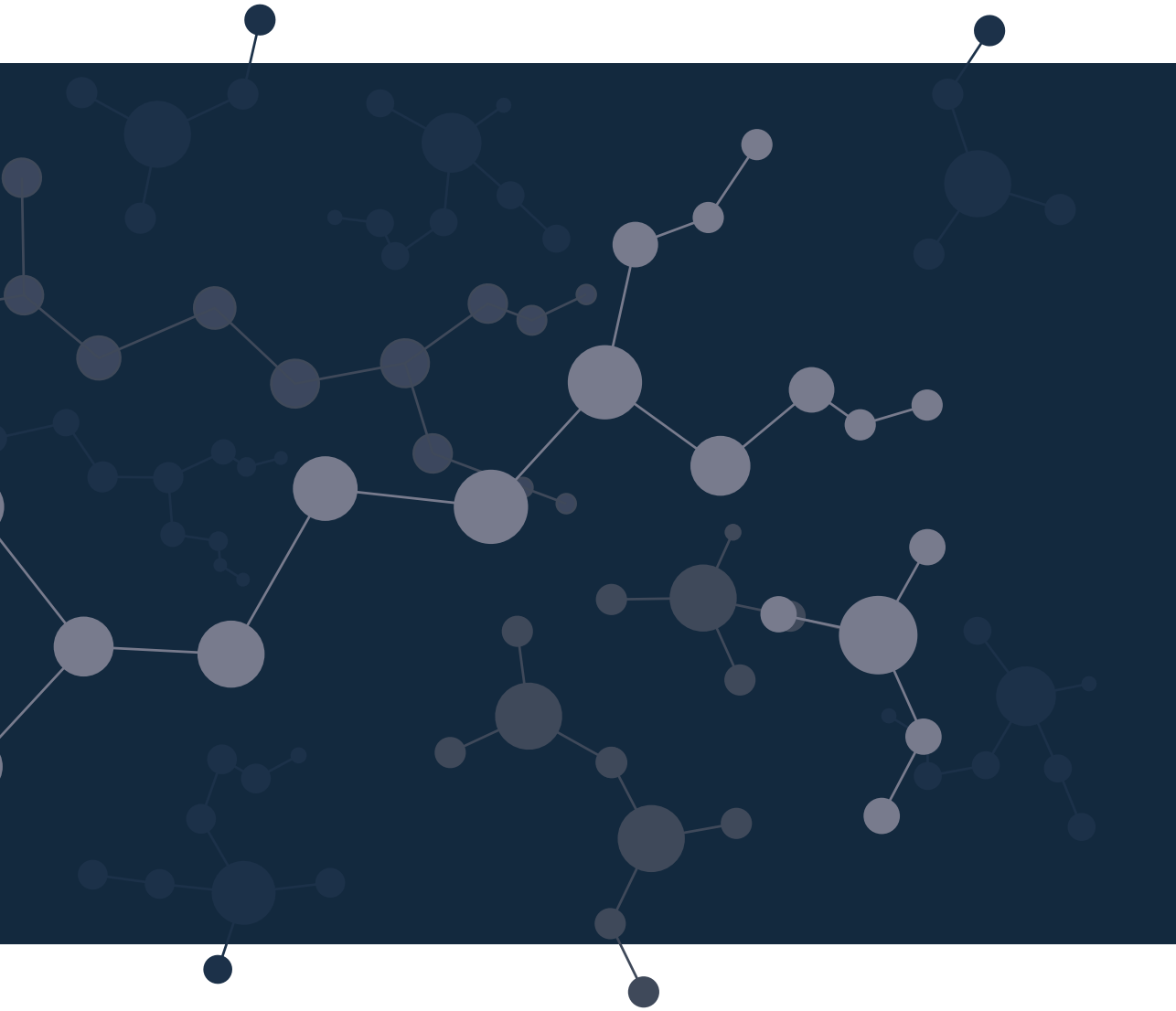

CHAPTER 3

A novel information criterion to elucidate a drug delivery mechanism from poly (acrylamide-co-2-hydroxyethyl methacrylate) reinforced with hydroxyapatite composite

Jomarien García Couce, Yaima Campos, Susana Torres, Gastón Fuentes, Eduardo Peón, Amisel Almirall, José Ángel Delgado, José C. Rodríguez-Cabello, Luis J. Cruz Ricondo

Polymer 2018, **158***: 279–288*

ABSTRACT

Hydrophilic composites of poly (acrylamide-co-2-hydroxyethyl methacrylate) reinforced with hydroxyapatite were synthesized, characterized and evaluated as drug delivery systems. The results show a strong dependence of the polymer composition, the degree of crosslinking and the homogeneity of the particles dispersion (filler or the mixed drug) in the characteristics that were analyzed. The mechanical properties were better while the swelling and the diffusion coefficient were worse than hydrogels with cefazolin of similar compositions. A new information criterion based on Bayesian criteria was used to elucidate the best fit. The drug diffusion into the medium was anomalous with more tendency to diffusional transport, indicating that under certain conditions zero-order diffusion could be achieved. This fact suggests that these materials could be used in the manufacture of medical devices for the controlled delivery of drugs and active or biological principles, significantly improving therapeutic procedures today.

Keywords: Composites, Drug delivery, Mathematical models

HIGHLIGHTS

- Hydroxyapatite-acrylic composites were designed to be used as drug release system.
- Incorporation of filler decrease the swelling and increase the mechanical properties.
- Swelling and release are mainly controlled by anomalous diffusion.
- The composite release 3 times more cephazolin than necessary in a plasma serum.
- The new information criterion should be very useful to take decisions during the work.

1. INTRODUCTION

The development of multifunctional polymer-based matrices for controlled drug delivery purposes has been a subject of intense research during the last six decades. After initial efforts to understand drug release mechanisms and to maintain a constant drug concentration in the blood, research moved into the advancement of polymers or hydrogels as smart materials where the delivery of the drug is triggered by changes in environmental factors.

The development of clinical products with the ability to deliver drug molecules to the right place and according to the patients' needs, has been a challenge that has gained more attention every day [1]. Ideally, controlled release systems can meet the criteria by maintaining the drug concentration within a therapeutic window for an extended period, minimizing dosage and frequency of administration.

Hydrogels are three-dimensional copolymeric mixtures crosslinked by covalent bonds and weaker cohesive forces, such as hydrogen bonds. They offer excellent potential as therapeutic systems due to diversity of both natural and synthetic material options and tunable properties. Also, crosslinked hydrogel networks can protect drugs from harmful environments, such as enzymes, low and basic pH and highly infected zones [2].

The hydrogels have been used in a wide range of biomedical applications which have been growing since both, synthetic and natural polymers can be used to reproduce the characteristics of soft tissue. Several natural polymers serve as raw materials to prepare hydrophilic copolymers from different sources of plant origin (cellulose, alginate) and of animal origin (chitin, chitosan). Their use in the biomedical field is extended to areas like ophthalmology, drug delivery, orthopedics and medical devices [3]. Virtually any water-soluble polymer can be formulated as a hydrogel. A feature that makes hydrogels truly unique as biomaterials for tissue regeneration is the possibility of fine tuning their mechanical characteristics (for example, elasticity) to match soft human tissue [4].

When used as drug delivery system (DDS) the mechanism of drug release includes a complicated diffusion pathway. The main effect is related to swelling and diffusion due to concentration gradients. It has been shown that drug release profiles can be tailored by various formulation conditions such as polymer property, combination of different polymers, surface coating, and the state of drug molecules in a solid phase [5].

On the other hand, the high density and slow biodegradability of some ceramic blocks sometimes limit tissue engineering purposes despite their excellent properties of bioactivity and bone induction and integration. To address these issues, macroporosity can be introduced often in combination with osteoinductive growth factors and cells. Ceramics are good carriers for drugs, in which release patterns are strongly dependent on the chemical consistency of the ceramic, type of drug and drug loading. Biodegradable polymers like polylactic acid, gelatin or chitosan are used as matrices for ceramic particles or as adjuvant to calcium phosphate cements. The use of these polymers can introduce a tailored biodegradation/drug release to the ceramic material [6].

It is well known that the incorporation of bioactive inorganic phases in hydrophilic polymers can enhance water ingress owing to the internal interfaces formed between the polymer and the more hydrophilic bioactive inclusions, hence enabling control of the degradation kinetics of scaffolds [7].

Many biodegradable materials have been evaluated as alternatives for DDS including protein-based materials (collagen, fibrin, thrombin, clotted blood) and synthetic polymers (polyanhydride, polylactide, polyglycolide, polyhydroxybutyrate-co-hydroxyvalerate, polyhydroxyalkanoate). Various forms and combinations of these materials have been investigated worldwide, characterizing their elution properties and performance in treating osteomyelitis in animal models [8].

In the biomedical field, the synthesis of hydroxyapatite (HAP)/polymer composite materials is of great interest for the development of biomaterials suitable to repair the skeletal system. There are several reasons to consider HAP powder as an appropriate reinforcement for organic polymers, HAP-filled composites using organic polymers have been largely used as bone cements, dental implants or bone replacement materials. One of the main advantages of HAP/polymer composites with respect to HAP biomaterials is the possibility to modulate biodegradability, bioactivity, and mechanical properties through changes in compositions. Furthermore, the presence of the polymer could improve the interfacial bonding of the composite with bone tissue [9].

Several authors report in literature the synthesis, characterization and evaluation of acrylic composites as drug delivery systems [10,11]. In the meantime, other authors add hydroxyapatite to these composites to improve their mechanical properties and bone affinity, and subsequently achieve a better control over the swelling and the drug delivery processes [12–14].

To select the best mathematical model is a child's play due to the multitude of criteria that exist [15,16]. But when models come from a same law, as in the case of the Fick's law of diffusion, all parameters prove to be very similar and the selection of the best model turns into a problem [17,18].

The information criteria are modern statistical parameters that consider any optimized statistical response (maximize or minimize), the number of parameters of the equation and the quantity of datapoints. Usually, the residual sum of squares is used as minimization and while the decrease of the value is higher the accepted opinion is that the adjustment of the examined model is better [15,16,19,20].

The aim of this study was − (i) prepare composites of poly(acrylamide-co-hydroxyethyl methacrylate) with HAP, (ii) study the influence of the composition in the hydrolytic and mechanical properties, and (iii) evaluate the capacity of the composites as drug controlled delivery systems of sodium cephazolin using a novel information criterion to make decisions.

2. EXPERIMENTAL SECTION

2.1. Materials

All chemicals were of analytical grade, used as received and they were purchased from Sigma-Aldrich Co. (Madrid, Spain) unless another supplier is declared. 2-Hydroxyethyl methacrylate (HEMA), acrylamide (AAm), $K_2S_2O_8$(PPS), N,N-methylen-bis-acrylamide (MBA), and sodium alginate (SAG, Nutra Sweet Kelco, San Diego, California, USA) were used for the composite preparation. Phosphate buffer saline (PBS) was used as medium to study drug release.

Sodium cephazolin (CFZ) was purchased from the Cuban Pharmaceutical industry (QUIMEFA, Havana, Cuba). The HAP was the inorganic phase in all the mixtures and was prepared by a wet neutralization reaction using CaO and H_3PO_4. The details of the HAP synthesis are described elsewhere [21].

2.2. Copolymerization reaction

Nine different formulations of acrylic composites were prepared according to a fractional experimental design (**Table 1**) $2^{4-1} = 2^3 = 8$ experiments adding a center with the variables: monomeric mixture ratio HEMA/AAm (shown as HEMA percent, reaching 100% adding AAm), MBA content (3–5%), dispersant concentration (SAG, 5–10%) and HAP content (36.5–43.5%).

Table 1. Experimental planning. 10% of cephazolin was used in all cases when decided

Level	HEMA	NNMBA[a]	Na(Alg)[a]	HAP[a]
-	25%	3%	5.0%	36.5%
0	50%	4%	7.5%	40.5%
+	75%	5%	10.0%	43.5%
		Experiments		
C0	0	0	0	0
C1	-	-	-	-
C2	+	-	-	+
C3	-	+	-	+
C4	+	+	-	-
C5	-	-	+	+
C6	+	-	+	-
C7	-	+	+	-
C8	+	+	+	+

[a] Percents calculated using the monomeric ratio (HEMA/AAm) as 100%.

The concentration of initiator (PPS) was 2% and HAP was chosen as alias variable according to the relation HAP = HEMA×MBA×SAG. Poly (HEMA-co-AAm) was prepared by free radical polymerization of the corresponding monomers mixtures in aqueous solution helped by the cross-linking agent (MBA), as it can be seen in **Fig. 1**

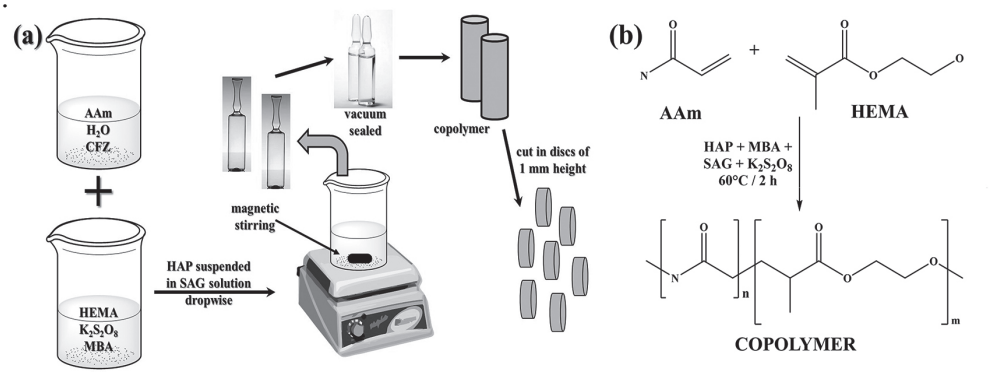

Fig. 1 - Composites preparation. (a) Schematic representation of the synthesis process. (b) Polymerization reaction of acryl monomers.

Glass ampoules were filled with the pre-composite fluid paste, and the polymerization was carried out at 60 °C for 2 h (Fig. 1). Then, the composite was extracted from the glass ampoule and cut into small discs of 1mm

thickness approximately, washed several times with distilled water, and dried under vacuum at 40 °C. The discs were polished using sandpaper # 400 to obtain a homogeneous thickness slightly below 1 mm, washed and dried again under same conditions [3].

2.3. Swelling behavior

The swelling behavior of the composites was determined by a weight method. The experiments were conducted at 37 °C, for which xerogel disc with (0.96 ± 0.04) mm average thickness. The samples were placed in 10 mL of distilled water and five experiments were carried out by measuring the weight gain (Sartorius BL 60S, Sartorius AG, Goettingen, Germany; **Eq. (1)**) as a function of immersion time for each composition.

$$W = \frac{M_t - M_0}{M_0} = 100\frac{M_t}{M_0} - 100 \qquad \textbf{(1)}$$

where W is the samples' swelling, M_t is the swelling sample mass at t time and M_0 is the dry sample mass at the time of initiating the study.

Measurements were done when the equilibrium hydration was reached, considered as when three consecutive determinations gave the same weight, or the swelling profile reached an asymptotic value.

2.4. Mechanical testing

The diametral tensile strength (DTS) was carried out using a load cell of 1 kN (InstronMicrotest 4505, Norwood, MA, USA). The average cross-section of the samples was 6mm width x 12mm height. A minimum of five samples were tested for each composition. A crosshead speed of 20 mm/min (3.3×10^{-4} m/s) was used until complete fracture. The samples for these tests were previously immersed in distilled water for 2 h at 37°C and dried over secant paper.

2.5. Drug delivery procedure

The composite with CFZ was prepared using the method proposed in Sect. 3.2, adding 10 wt% of antibiotics to the pre-composite paste. The *in vitro* release of CFZ from composites was carried out at 37°C by immersion in 10 mL of phosphate buffer saline (PBS) for 5 h at pH=7.4. PBS was collected and replaced with equal volume of fresh PBS at scheduled time intervals of 5 min during the first 30 min, 10 min up to the first hour, 30 min up

to 3 h, and 1 h to the end at 6 h. The released cephazolin was measured at 272 nm using a UV–Visible spectrophotometer (Cintra GBC 10/20/40, Sydney, Australia). These experiments were carried out in quintuplicate. The calibration curve was made using cephazolin solutions with different known concentrations.

2.6. Mathematical modelling of the drug release kinetics and mechanisms

Analysis of the sodium cephazolin release kinetics from several poly (HEMA/AAm) composites was performed by stepwise refinement of Fick's second law of diffusion under initial and boundary conditions equivalent to those of the assays carried out in this work [22].

Five diffusion models were considered to fit the experimental data. First, the Higuchi model (**Eq. 2**) that related the release mass vs thesquare root of time [23]. In addition, it was calculated the diffusion coefficients, D (**Eq. 3**, from slope of linear fit, kH, of **Eq. 2** and compared to the sodium cephazolin diffusion coefficient in water solution at 37°C from similar copolymers of 3×10^{-7} cm^2/s [24].

$$\frac{M_t}{M_0} = k_H\sqrt{t} \qquad \textbf{(2)}$$

$$D = \frac{\pi h^2 k_H^2}{16} \qquad \textbf{(3)}$$

where M_t/M_0 is the fractional drug release, t is the release time and k_H is a kinetic constant.

The second model (KP) tested was reported by Korsmeyer and Peppas through **Eq. 4** [25].

$$\frac{M_t}{M_0} = k_D t^n \qquad \textbf{(4)}$$

where k_D is a kinetic constant and n is the diffusional exponent that can be related to the drug transport mechanism. For a thin hydrogel film of n = 0.5, the drug release mechanism is considered as Fickian diffusion. While n = 1, Case II transport occurs, leading to zero-order release. And for a value between 0.5 and 1, anomalous transport is stablished [26].

The third model is described also by the Ritger and Peppas equation, Eq. 5, but with exponent n fixed to 0.5 [22]. The first term of this equation represents the contribution of Fickian diffusion and the second term refers to the macromolecular relaxation contribution on the overall release mechanism; k_D and k_R means kinetic constant of each process (diffusion and relaxation):

$$\frac{M_t}{M_0} = k_D\sqrt{t} + k_R t \quad \textbf{(5)}$$

The fourth model was described by Lindner and Lippold (**Eq. 6**), and the *b* term represents the burst effect associated to drug delivery from the matrix surfaces [27]:

$$\frac{M_t}{M_0} = k_D t^n + b \quad \textbf{(6)}$$

The fifth model is based on the Peppas–Sahlin equation (**Eq. 7**), which accounts for the coupled effects of Fickian diffusion and Case II transport [28] but with the possibility to fit the value of *n*:

$$\frac{M_t}{M_0} = k_D t^n + k_R t^{2n} \quad \textbf{(7)}$$

In addition, after a certain period of time, a pseudo second order equation previously reported [3,29], **Eq. 8**, was used in order to predict the maximum swelling or release from these matrixes:

$$\frac{t}{M_t} = \frac{t}{M_\infty} + \frac{1}{k_1 M_\infty^2} \quad \textbf{(8)}$$

Using the estimated parameters k_D and k_R, obtained from fitting the experimental data to **Eq. 7**, the ratio of Fickian (*F*) and relaxation (*R*) contributions were calculated with **Eq. 9** [28,30] and plotted vs M_t/M_∞ as:

$$\frac{R}{F} = \left(\frac{k_R}{k_D}\right) \times t^n \quad \textbf{(9)}$$

2.7. Statistical analysis

Data are reported in graphics as mean ± standard deviation (SD) from triplicate measurements for each composite and parameters are reported in tables as value ± standard error (se) unless stated otherwise. From **Eq. 2** to **Eq. 6**, the mathematical evaluation is valid only for the first 60% of the drug release [23,31,32]. Experimental data were analyzed by linear and nonlinear least-squares regression, using OriginPro 2018 (OriginLab Corp, Northampton, MA, EEUU).

As statistical criterion to distinguish the models that best described the data, the residual sum of the squares (*RSS*) was calculated. The model with the minimal *RSS* value was considered the better fit model. However, since a larger number of model parameters could lead to a higher probability of obtaining a smaller RSS value, it was necessary to use a discriminatory criterion that was independent of the number of parameters that each model had [19,20]. For this reason, a new Bayesian information criterion (BIC_N) was applied. The BIC_N was defined as:

$$BIC_N = N \ln \frac{RSS}{N-1} + p \ln \frac{N-p}{\pi p} \qquad \textbf{(10)}$$

where *N* is the number of experimental data points and p is the number of parameters. The model that showed the smallest value for the BIC_N, **Eq. 10**, was considered as the model that statistically best describes the drug release profile [33]. Additionally, the fit of the predicted curve to the experimental data and the validity of the calculated parameters was examined.

3. RESULTS AND DISCUSSION

The samples preparation by radical copolymerization of HEMA and AAm in presence of HAP and sodium alginate and the effect of composition on the properties of composite was evaluated. In addition, the incorporation of MBA will give chemically cross-linked composites with improved mechanical properties due to the additions of HAP [34].

3.1. Swelling studies

The swelling behavior of a polymeric system has a great importance when it is applied in the biomedical field as its hydration degree influences on

the surface properties and internal chains movement, on its mechanical properties and on the type of solute transport mechanism through the hydrogel. The equilibrium hydration degrees are slightly different from the maximum swelling, $W_{eq} \neq W_{max}$, and was attained at similar times for all studied formulations.

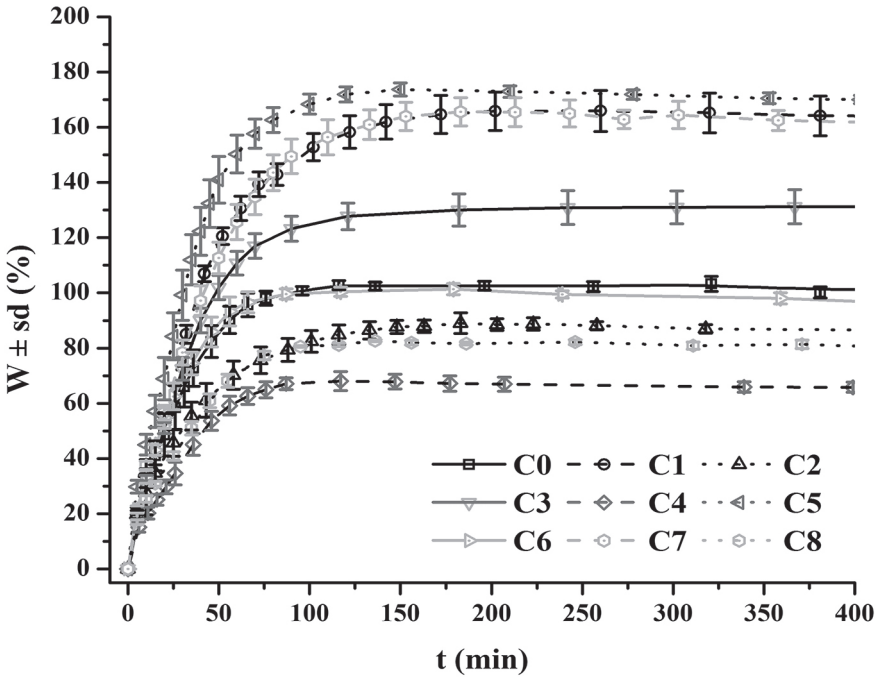

Fig. 2 - Swelling isotherm profiles (37°C) of the composites

Fig. 2 shows the swelling profile of samples. It was observed that those identified with odd numbers have more swelling that those with even numbers. It could be explained by the more hydration sites in case of acrylamide than hydroxyethyl methacrylate, two ($-NH_2$) by one (OH^-) as it can be seen in **Fig. 1** (right). Besides, it can be observed that swelling maximum value for all samples was reached in a range between 100 and 150 min. After that, the swelling value descends among 2 and 13% in all samples up to reach the equilibrium. The presence of HAP in a very short range of variation could be led to a water absorption of its agglomerates inside the copolymer in comparison with other similar materials [3]. This is one of the causes of the difference between the equilibrium hydration degree and maximum swelling in all the samples.

To know the water transport mechanism, the initial swelling data were fitted using **Eq. 4** in its linear form:

$$\ln \frac{W_t}{W_\infty} = \ln k_w + n \ln t \qquad \textbf{(11)}$$

where W_t is the mass of water uptake at time t, W_∞ is the equilibrium water uptake, k_W is a characteristic constant of the macromolecular network or particle system, and n is the diffusional exponent which is indicative of the transport mechanism. This power law has first been introduced in the pharmaceutical field by Peppas in 1985 and has become known as the "Peppas' equation". It is valid for the first 60% of the normalized drug release [35].

The values of n have a fluctuation between 0.53 and 0.71 (**Table 2**), indicating double management of water uptake, but with more influence of diffusion process than chain relaxations. It was a very good fitting of the swelling versus time data to the pseudo second-order kinetic equation proposed in the literature was observed because all the values of R^2 are higher than 99.8%, which explains accurately the variability in swelling from this model (**Table 2**). A good agreement among the values from the swelling isotherm and the values predicted by **Eq. 7** modified was observed. This equation allows to predict the equilibrium swelling degree at ending stages with a minimum data [29].

Table 2 - Kinetics parameters of swelling process (α=0.05).

Samples	Eq 3.11			Fig. 1		Eq 3.7	
	$n \pm$ se	$k_W \pm$ se	R^2_{fit} (%)	W_{eq}†	W_{max}†	W_{max}‡	R^2_{fit} (%)
C0	0.617 ± 0.008	8 ± 1	99.94	95 ± 2	103 ± 3*	96.7 ± 0.8*	99.79
C1	0.7 ± 0.1	8 ± 1	95.55	157 ± 9	166 ± 7	160 ± 3	99.88
C2	0.532 ± 0.009	8 ± 1	99.88	82 ± 1	89 ± 4*	82.4 ± 0.6	99.93
C3	0.71 ± 0.06	6 ± 1	98.48	132 ± 6	133 ± 7	133 ± 4	99.96
C4	0.63 ± 0.02	5 ± 1	98.99	65.2 ± 0.4	68 ± 3	65.7 ± 0.3	99.97
C5	0.592 ± 0.002	11 ± 1	99.99	163 ± 2	174 ± 2*	166 ± 6*	99.89
C6	0.67 ± 0.02	7 ± 1	99.71	87.2 ± 0.6	101 ± 2*	88 ± 2*	99.87
C7	0.66 ± 0.06	8 ± 1	98.65	156 ± 3	166 ± 5	157 ± 3	99.95
C8	0.57 ± 0.01	7 ± 1	99.70	73 ± 4	82.7 ± 0.4*	73.5 ± 0.8*	99.88

From experimental data, ‡from Eq (3.7) substituting the mass ratios by swelling ratios; *statistical difference at same row (α = 0.05).

Finally, **Eq. 12** shows a strong dependence on the three main effects with a R^2=96.94%. It can be observed that the influence of the variables is related

with the interfering effect of the monomeric composition and cross-linking content and synergic effect for the SAG content in that order.

$$W = 120 - 37\,HEMA - 10\,MBA + 8\,SAG \qquad (12)$$

It should be remarked that the dispersant had an opposite effect than the other two variables. It can be explained by the "apparent internal contest" between the increase of viscosity and solubility of the sodium alginate. In the experimental range, the dispersant hydrophilicity prevails over its capability of change of the ion's concentration of the reaction medium (see **Table 2** and **Fig. 2**).

3.2. Mechanical properties

As expected, the addition of load improves the mechanical capacity of the materials. **Fig. 3** illustrates the diametral tensile strength values in the composites hydrated for 2 h at 37°C. The average strength showed an approximate value of 800 kPa, twenty times higher than other similar materials. In this case, it can be observed that when the concentration of the less hydrophilic monomer (HEMA) is increased, the compressive strength of the material increases too. On the contrary, when the amount of alginate sodium increases, the DTS decreases [3].

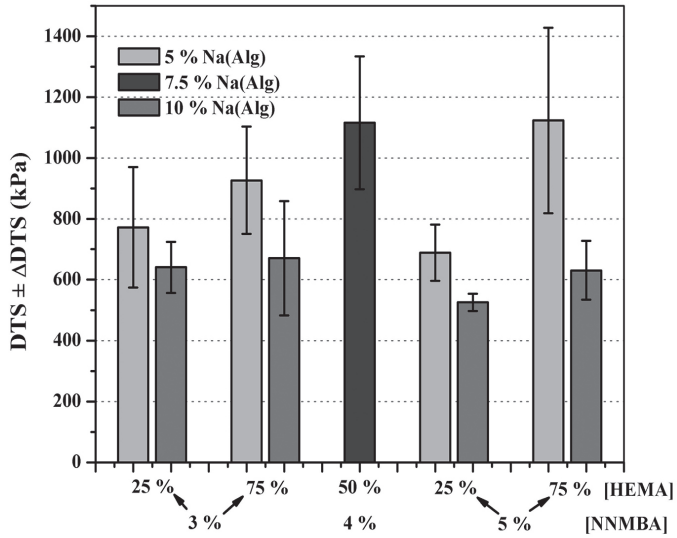

Fig. 3 - Bars graph of DTS for all samples (n > 5).

For both cases (concentrations of SAG and HEMA), the explanation is very similar. An increase in the alginate amount, a soluble natural polymer generates more carbohydrate units' link sites for hydrogen bonding, giving the matrix the possibility to maximize its swelling that makes it a little more porous, creating a relaxation between the chains that does not benefit the mechanical strength.

The interpretation of the phenomenon with HEMA goes through similar channels, but in this case the samples with the highest amount of HEMA swell less than the similar ones with a small quantity. Moreover, the mechanical properties are better in both cases due to the decrease of the number of binding sites for hydrogen bonding.

3.3. Statistical evaluation of mathematical models

Drug release from the different examined formulations occurred during the slight erosion of the surface matrix in contact with PBS at pH=7.4. At the end of the release process the matrix remains intact, with only a small mass loss attributable to the drug released and the creation of small surface pores through which PBS penetrates to dissolve the drug and remove it from the matrix. The release profiles of each matrix are shown in **Fig. 4**. As expected, they have a similar shape to the swelling profiles, skipping the relationship between the two properties. However, there are changes in the behavior of samples that can be attributed mainly to the change in medium, that is, distilled water for swelling process and PBS for drug delivery.

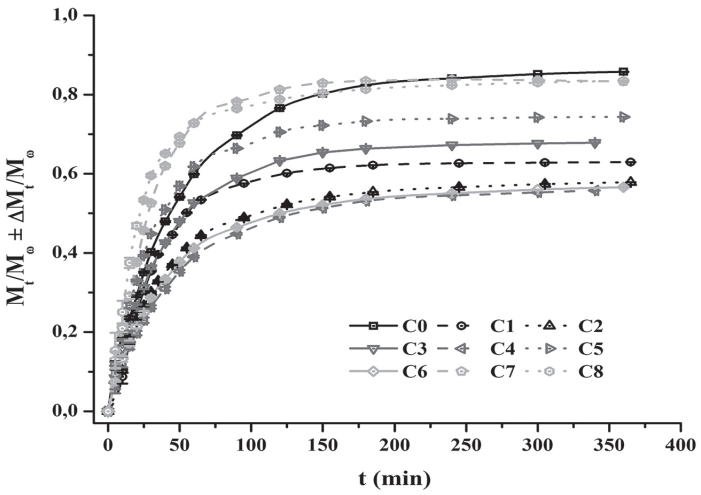

Fig. 4 - Release profiles of matrixes (n=5).

The salt concentration of the buffer helps to control the equilibrium in the swelling (hydroxyapatite is part of the composite), diffusion, and therefore the release in certain compositions. All the process can be considering as an osmosis, simulating the main parts of the process such as cell (matrix), cell inside (interior of the matrix with drug) and cell outside (PBS release medium). These changes in position of some release profiles with respect to swelling profiles announce, perhaps, an irregular behavior in the matrices. An extremely important factor to remark is that the solubility and concentration of drug in the carrier matrix do not exist in the composites prepared for the swelling process.

Depending on the composition of a device (type of polymer, drug loading, additives) and geometry (size and shape), numerous mass transport phenomena and chemical reaction phenomena affect the resulting drug release kinetics [36].

The release experimental data was fit to **Eq. 11** in order to elucidate variations in the kinetic parameters with respect to the swelling study without drug (**Tables 2** and **3**) caused by the use of drug in formulations and the change in release medium, water by PBS medium. It determines which of the phenomena could be affecting the drug delivery process.

Table 3 - Kinetics parameters of drug delivery process and diffusion coefficient for cephazolin delivery process in PBS at 37 °C. ($D \times 10^7$ cm^2/s, α=0.05).

Sample	Eq. 11			Eq. 2	Eq 3	
	$n \pm$ se	$k_W \pm$ se	R^2_{fit}	$k_H \pm$ se	$D \pm$ se	R^2_{fit}
C0	0.68 ± 0.01	0.039 ± 0.002	99.74	0.072 ± 0.002	1.59 ± 0.09	99.23
C1	0.93 ± 0.05	0.015 ± 0.003	98.70	0.063 ± 0.003	1.2 ± 0.1	98.08
C2	0.66 ± 0.03	0.032 ± 0.003	98.81	0.054 ± 0.002	0.87 ± 0.05	99.24
C3	0.78 ± 0.02	0.025 ± 0.002	99.43	0.064 ± 0.002	1.25 ± 0.08	99.04
C4	0.69 ± 0.02	0.025 ± 0.001	99.61	0.048 ± 0.001	0.68 ± 0.04	99.34
C5	0.82 ± 0.04	0.028 ± 0.003	98.66	0.078 ± 0.002	1.8 ± 0.1	99.11
C6	0.70 ± 0.02	0.025 ± 0.002	99.47	0.051 ± 0.001	0.78 ± 0.04	99.33
C7	0.79 ± 0.02	0.035 ± 0.002	99.66	0.089 ± 0.005	2.4 ± 0.2	98.15
C8	0.80 ± 0.03	0.042 ± 0.003	99.39	0.101 ± 0.005	3.1 ± 0.3	98.56

It can be clearly seen that the value of diffusional exponent increased while the values of the swelling constant decreased by more than one order. In the case of diffusional exponent, it can be attributed to the inclusion of the drug and the appreciable ionic concentration on medium with respect to

water. This is the cause of the anomalous diffusion process, a competitive process between the two classical diffusion types, the Fickian and type II due to the interactions of ions of the PBS solution and the drug molecules that are dissolved and removed from the matrix. At the same time, the kinetic constant reflects this effect when the equilibrium is reached at 100 min in swelling and 175 min in release. Most of the phenomena described before can affect these matrixes and they explain the changes between swelling process and drug delivery, mainly to the matrix composition and the way to prepare it [36]. The release experimental data was fitted to Eq. 4.2 to obtain the cephazolin diffusion coefficient (**Eq. 3**) in PBS and compare it with those reported in literature.

The diffusion coefficients of the drug are lower than those ones reported for cefazolin in all samples except the C8 (**Table 3**). This coefficient decrease could primarily be due to inclusion of hydroxyapatite within the hydrogel, which establishes no soluble cores that can become agglomerates and cause a slowdown in the process of molecular diffusion by interactions between the drug and calcium phosphate nuclei. In addition, the release PBS medium could cooperate synergistically to this process by establishing ionic balance once the matrix is fully swelling. These two reasons might explain the increased values of the adjusted coefficient of determination in **Table 3** with respect to **Table 2**.

To discuss the possible mechanism of drug delivery from matrixes to solution, the obtained data was fitted to **Eqs. 4-7** (Peppas' models). The fitting was globally good as shown in **Table 4**, according to the values of the adjusted coefficients of determination (R^2_{fit}).

The values of n obtained from **Eq. 4** (**Fig. S1**) were in the first part of anomalous diffusion range (0.50–0.77), according to previous results of swelling. This fact confirms that the diffusion, at least, is one of the main processes that lead the drug delivery. This was confirmed by BIC_N values of samples C0 and C3 which are separated in almost 20 units, which means three orders higher in differentiating magnitude (**Table 4**) instead of R^2_{fit} values whose differences reach four centesimal places between them. It is obviously affected by the number of experimental data used and the residual sum of squares, since, in this case, the number of parameters is the same. The values of the kinetic constants of the release process are proportionally lower than those in the swelling process as with other parameters, due to the change of environment and molecular interaction between the drug and interior nuclei of calcium phosphate and polymeric crosslinking nodes. A similar explanation applies if the results of **Eq. 5** (**Fig. S2**) are analyzed. The values of k_D are one order or four times higher than k_R, indicating the supremacy of the diffusion mechanism

associated to $t^{½}$ over the relaxation process of the polymer chains, associated to t [3,22,28]. In fact, some of the values of k_R, although small, are negative, therefore indicating an interfering effect on the model. For this model, it can be seen that the best values in descending order of the determination coefficient and sum of the square residuals are for C0, C7 and C8 samples. However, the best values of BIC_N in the same order are samples C6, C4 andC2. It is necessary to consider that between C0, C7 and C8 there are only 0.22 units of percent in R^2_{fit}, while BIC_N is separated by 3 units (**Table 4**), as explained before. The Peppas' equations, derived from Higuchi theory, require their application in the ascending line at the beginning of the delivery process (usually $M_t/M_\infty \leqslant 0.6$), because they are based on real diffusion only dependent on the penetration of fluids through the inter-polymeric channels that are created during the swelling process. In this model, the statistical criteria, as in the first case, do not match because the equation to calculate BIC_N is multiplied by the data number of points. Due to its low ability to release (**Table 4**), C6 formulation reaches a maximum under the ratio required for the implementation of Ritger and Peppas model [22,37]. In case of **Eq. 6** (**Fig. S3**), b is the y-axis intercept, characterizing the burst effect [27,38]. It can be observed in **Table 4** that all the b values are negative and with non-statistical significance. This leads us to think that in our composites the inclusion of the burst effect in the equation may occur from the physical point of view; it would be able to help the phenomenology of the problem, but mathematically it is not relevant. In fact, when eliminating it, we were left with Peppas's classical equation (**Eq. 4**) and if a comparison of R^2_{fit} is made in all cases, **Eq. 4** will better fit than **Eq. 6**, but if the BIC_N, is considered then **Eq. 6** adjusts better than **Eq. 4**. In general, it is important to consider that the information criteria are strongly "weighed" by the number of data and parameters [19,20]. It is clearly seen in the values reported in **Table 4**, that **Eq. 7** (**Fig. S4**) is the model that best fits all the experimental data, not only for the highest values of the determination coefficient but also because of the smaller RSS and BIC_N. The n values closer to unity confirm the enormous influence of the medium change, being the drug release dependent linear on time, but the diffusion mechanism continues as dominant with values in the range of 0.58 and 0.97. It is important that all k_1 values are positive and two or three orders larger than the k_2 values, which are all negative, which confirms the greater influence of the diffusion process over release process from the matrixes. The results of this model show exactly the same coefficients of determination for the C7 and C8 samples, which also have fairly similar RSS values. However, and despite that they only differ in the number of experimental data in one unit, the BIC_N manages to separate them by almost seven units. This is similar to previous results where the best settings for the coefficient of determination and the residual sum of squares match, but not the best by BIC_N. C3, C5 and C0 samples in that order were the best fits for R^2_{fit} and RSS while C3, C4 and C6 samples were the best for BIC_N.

Table 4
Kinetic and statistical parameters of fitting to Eqs. (4)–(7) (α = 0.05). In the first column, between parentheses, the number of iterations for non-linear regression. In the first row, between keys the number of experimental points for each data according to $M_t/M_\infty \times 0.6$. For Eq. (8) (linear regression) all the samples use the same number of experimental points (between keys near to equation number).

Eq. #	Parameters	C0 {10}	C1 {17}	C2 {17}	C3 {12}	C4 {17}	C5 {10}	C6 {17}	C7 {8}	C8 {7}
4(7)	n	0.65 ± 0.02	0.29 ± 0.04	0.31 ± 0.03	0.51 ± 0.04	0.35 ± 0.03	0.63 ± 0.04	0.33 ± 0.03	0.77 ± 0.03	0.75 ± 0.04
	k_D (min^n)	0.043 ± 0.002	0.13 ± 0.03	0.11 ± 0.02	0.060 ± 0.009	0.08 ± 0.01	0.049 ± 0.007	0.09 ± 0.01	0.038 ± 0.003	0.048 ± 0.005
	R^2_{fit} (%)	99.77	85.48	91.39	96.90	93.77	98.70	92.79	99.66	99.56
	RSS	0.00066	0.09175	0.04119	0.01257	0.03166	0.00435	0.03682	0.00089	0.00103
	BIC_N	−94.69	−86.00	−99.62	−80.36	−104.09	−75.86	−101.52	−71.83	−61.15
5 (4)	k_D ($min^{-0,5}$)	0.049 ± 0.003	0.078 ± 0.004	0.066 ± 0.002	0.064 ± 0.006	0.058 ± 0.002	0.056 ± 0.007	0.062 ± 0.002	0.038 ± 0.006	0.047 ± 0.008
	k_R (min^-)	0.0039 ± 0.0005	−0.0024 ± 0.0003	−0.0019 ± 0.0002	−2 ± 7	−0.0015 ± 0.0002	0.003 ± 0.001	−0.0017 ± 0.0002	0.010 ± 0.001	0.012 ± 0.002
	R^2_{fit} (%)	99.62	93.80	97.11	96.92	97.69	98.27	97.73	99.52	99.40
	RSS	0.0011	0.03919	0.01384	0.01248	0.01177	0.00580	0.01160	0.00126	0.00139
	BIC_N	−89.61	−100.46	−118.16	−80.45	−120.91	−72.99	−121.16	−69.07	−59.05
6 (8)	n	0.64 ± 0.02	0.27 ± 0.06	0.29 ± 0.05	0.48 ± 0.05	0.32 ± 0.05	0.60 ± 0.05	0.30 ± 0.05	0.76 ± 0.04	0.74 ± 0.05
	k_D(min^n)	0.044 ± 0.005	0.16 ± 0.06	0.13 ± 0.04	0.07 ± 0.02	0.10 ± 0.03	0.06 ± 0.01	0.12 ± 0.04	0.039 ± 0.006	0.049 ± 0.009
	b	−0.003 ± 0.009	−0.04 ± 0.08	−0.03 ± 0.05	−0.03 ± 0.03	−0.04 ± 0.04	−0.02 ± 0.02	−0.04 ± 0.05	−0.01 ± 0.01	−0.01 ± 0.01
	R^2_{fit}	99.75	84.82	91.05	96.80	93.76	98.61	92.72	99.60	99.45
	RSS	0.00065	0.08954	0.03997	0.01166	0.02958	0.00406	0.03470	0.00088	0.00102
	BIC_N	−96.27	−86.97	−100.68	−82.33	−105.80	−77.93	−103.08	−73.73	−63.33
7 (12)	n	0.77 ± 0.04	0.60 ± 0.04	0.58 ± 0.03	0.81 ± 0.02	0.63 ± 0.02	0.92 ± 0.03	0.59 ± 0.02	0.93 ± 0.06	0.97 ± 0.07
	k_D (min^n)	0.033 ± 0.003	0.051 ± 0.009	0.047 ± 0.006	0.027 ± 0.002	0.035 ± 0.003	0.025 ± 0.002	0.043 ± 0.004	0.027 ± 0.004	0.032 ± 0.005
	k_R (min^{-2n})	(-32 ± 3) × 10^{-5}	(-9 ± 4) × 10^{-4}	(-9 ± 2) × 10^{-4}	(-28 ± 4) × 10^{-5}	(-55 ± 9) × 10^{-5}	(-25 ± 4) × 10^{-5}	(-8 ± 2) × 10^{-4}	(-22 ± 4) × 10^{-5}	(-36 ± 9) × 10^{-5}
	R^2_{fit} (%)	99.86	95.32	98.05	99.81	99.37	99.84	98.86	99.78	99.78
	RSS	0.00036	0.02756	0.00869	0.00070	0.00301	0.00046	0.00546	0.00048	0.00041
	BIC_N	−102.29	−107.00	−126.62	−116.15	−144.64	−99.78	−134.52	−78.57	−69.70
8	M^a_∞(mg)	17.150 ± 0.004	12.5820 ± 0.0005	11.573 ± 0.002	13.573 ± 0.002	11.149 ± 0.002	14.876 ± 0.001	11.320 ± 0.007	16.666 ± 0.002	16.703 ± 0.005
	M^a_∞(%)	85.75 ± 0.02	62.910 ± 0.003	57.864 ± 0.009	67.864 ± 0.008	55.74 ± 0.01	74.378 ± 0.005	56.60 ± 0.03	83.33 ± 0.01	83.52 ± 0.03
	M^b_∞(mg)	19.5 ± 0.2	14.1 ± 0.4	12.9 ± 0.2	15.2 ± 0.2	12.6 ± 0.1	16.3 ± 0.2	12.6 ± 0.1	18.2 ± 0.3	17.6 ± 0.2
	M^b_∞(%)	98 ± 1	71 ± 2	65 ± 1	76 ± 1	63.0 ± 0.5	82 ± 1	63.0 ± 0.5	91 ± 2	88 ± 1
	$k_D \times 10^4$ $(min\ mg)^{-1}$	12.9 ± 0.8	22 ± 4	22 ± 2	20 ± 2	19.8 ± 0.8	24 ± 2	22.5 ± 0.9	24 ± 3	33 ± 3
	R^2_{fit}(%)	99.76	98.58	99.70	99.69	99.88	99.69	99.91	99.56	99.88
	BIC_N	−40.45	−1.39	−23.55	−29.17	−38.74	−30.25	−41.88	−28.28	−48.26
	[Z] (μg/mL, 90 min)	1394 ± 2	1150.7 ± 0.9	978 ± 3	1178 ± 1	897 ± 5	1329 ± 1	929 ± 3	1564 ± 3	1529 ± 3

[a] from experimental data (see Fig. 4); [b] from Eq. 7.

Summarizing, in the use of these models it is important to assess competition of drug dissolution and removal to the release movement of the solvent against relaxation of the polymer chains during the swelling process, greatly compromised by the material crosslinking and the addition of hydroxyapatite as filler. Hence, drug solubility is a variable of remarkable importance in the analysis of the drug release process [22,26,28,35,37]. All the experimental values were fitted to **Eq. 7** [29], to predict what would be the maximum release percent that each matrix would reach. **Table 4** shows those values and the percentage achieved for each sample. Clear differences can be seen between the masses released at endpoint. Experimentally proved, they are always being lower than those predicted by **Eq. 7**. This can be attributed to the fact that the release process was stopped aftr 6 h. Another reason could be the equilibrium reached. Note that the slopes observed in the upper part of the profile (**Fig. S1**) lead to the conclusion that this process is not complete.

In fact, there can be a variation between 5 and 13% calculated between the percentages in both methods, showing that remains drug able to be transferred to the physiological medium. However, **Eq. 8** (**Fig. S5**) is very useful to predict the maximum percent of matrixes released, considering that the identified slopes are small.

Finally, samples delivered between 55 and 85% after 6 h of study while the prediction to be released was between 63 and 98% at the end. Cephazolin minimum inhibitory concentration (MIC) for Gram(+) sensitive is 0.1–1.0 mg/mL. It should reach a maximum plasma concentration of 185 μg/mL between 60 and 120 min after administration [39]. According to these results, in that middle range of time (90 min) the concentrations of cephazolin from all the matrixes were at least four times higher than the value reported (see last row in **Table 4**).

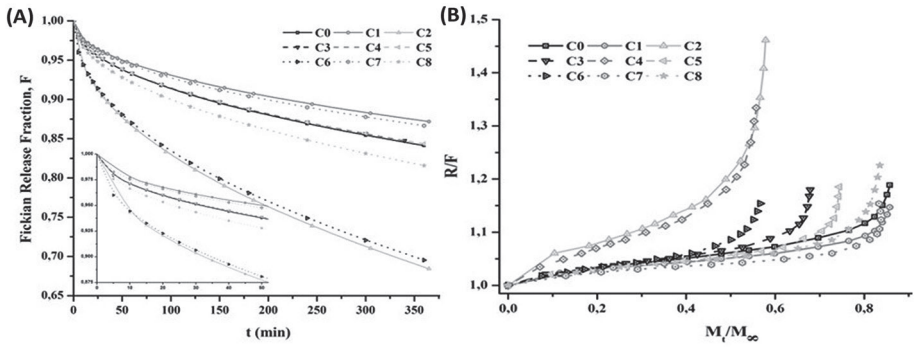

Fig. 5 - Fickian release fraction, F vs t (a) and R/F ratio vs the fraction of the drug released from composites (b)

Equation 9 must be used because it is difficult to give an exact answer concerning the importance of the Fickian or Case-II mechanism just from determination of n, k_1 and k_2. **Fig. 5** indicates the Fickian release fraction vs time, and the ratio between the relaxation contribution (R) and the diffusional contribution (F) during drug release process. Both graphs give an approximation of the behavior of the release process and the most influential mechanisms in it.

Since the values of k_R are at least three orders minor than k_D, a curve with an exponential decrease is shown in **Fig. 5a**, being the value of diffusional exponent dependent on the matrix composition the main factor of differentiation. The profiles are similar to that obtained by Peppas and Sahlin in their pioneering article on these issues [28]. If we look at **Fig. 5b**, it can be seen exactly up to 50–60% of the release process, the relationship ratio R/F remains close to unity, which reinforces the criteria of an anomalous diffusion with a tendency to a relaxation of polymer chains control at the end of the process [28,30].

4. CONCLUSIONS

Hydroxyapatite-poly(HEMA/AAm) composites were designed and synthesized to be used as novel controlled drug release devices. The results obtained during experimental and mathematical analysis showed that the incorporation of hydroxyapatite decreases the swelling capacity of these materials, while the mechanical properties significantly increase compared to the similar composition in hydrogels. In turn, the polymer composition proves to be the most important factor in almost all analyzed properties, except for the synergy of crosslinking and the nucleation sites provided by the calcium phosphate. Both, the swelling and release processes, are mainly controlled by anomalous diffusion but with clear trends to diffusional transport, especially in the case of release, where apparently, drug addition and change of medium (PBS by water) make the diffusion more dependent on the cross-linked polymer chains. The quantity of drug released to the medium was 3 times higher than necessary range for cephazolin in biological serum. Additionally, a novel statistical criterion allowed to select the best formulations or mechanisms according to the statistical analyzes performed. It can be conclusively said that these matrices could be used as materials for manufacturing medical devices to help a micro-localized, uniform and extended delivery of drug in bone tissue.

Acknowledgements

The authors would like to acknowledge the financial support from the European Union through the Erasmus PLUS project code NL01-KA 107-008639 for J. García and Y. Campos (doctoral fellowship) and G. Fuentes and A. Almirall (staff mobility). Also, was partially supported by the Erasmus MUNDUS LINDO post-doctoral fellowship; code ML14PD1157, from the European Union for Gastón Fuentes. The authors wish to thank Miss María José López Carrero for her invaluable help and suggestions.

Supplementary figures

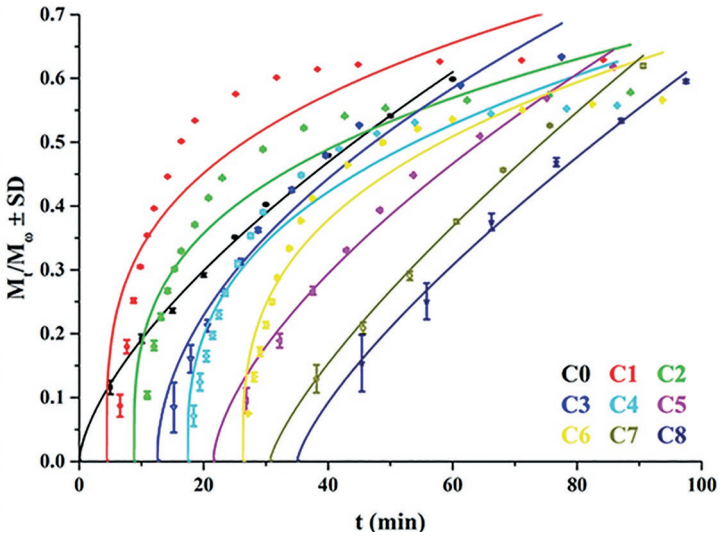

Fig. S1 - Fitting of appropriate experimental data ($M_t/M_\infty \leqslant 0.6$) to Eq. 4 (Korsmeyer & Peppas). C0 (n=10), C1 (n=17), C2 (n=17), C3 (n=12), C4 (n=17), C5 (n=10), C6 (n=17), C7 (n=8), C8 (n=17), R^2 = 99.63 %. The data of each sample are displaced by the abscissa to avoid overlapping of points and fitting curves.

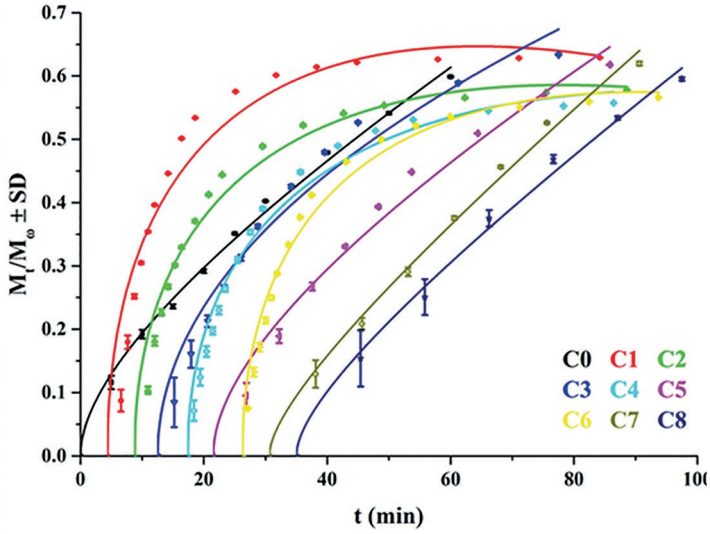

Fig. S2 - Fitting of appropriate experimental data ($M_t/M_\infty \leqslant 0.6$) to **Eq. 5** (Ritger & Peppas). C0 (n=10), C1 (n=17), C2 (n=17), C3 (n=12), C4 (n=17), C5 (n=10), C6 (n=17), C7 (n=8), C8 (n=17), R^2 = 99.50 %. The data of each sample are displaced by the abscissa to avoid overlapping of points and fitting curves.

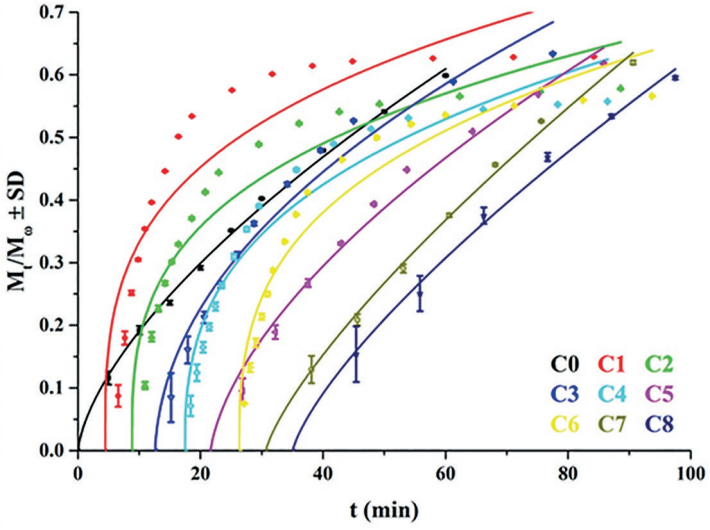

Fig. S3 - Fitting of appropriate experimental data ($M_t/M_\infty \leqslant 0.6$) to **Eq. 6** (Lindner & Lippold). C0 (n=10), C1 (n=17), C2 (n=17), C3 (n=12), C4 (n=17), C5 (n=10), C6 (n=17), C7 (n=8), C8 (n=17), R^2 = 99.63 %. The data of each sample are displaced by the abscissa to avoid overlapping points and fitting curves

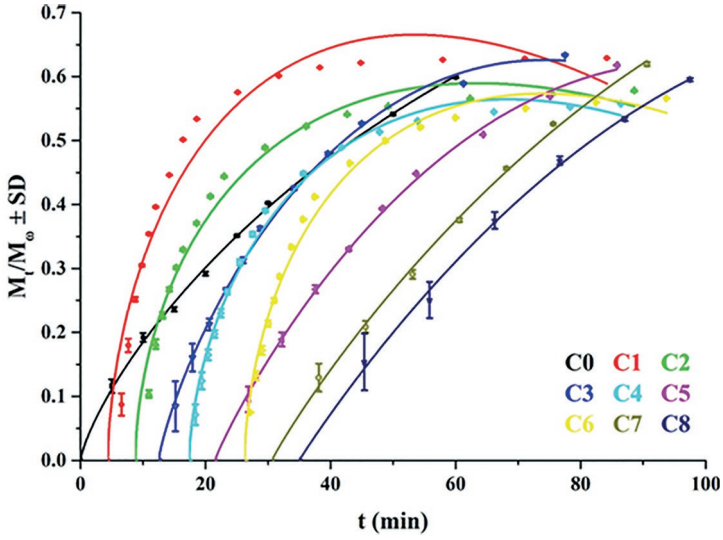

Fig. S4 - Fitting of appropriate experimental data ($M_t/M_\infty \leqslant 0.6$) to **Eq. 7** (Peppas & Sahlin). C0 (n=10), C1 (n=17), C2 (n=17), C3 (n=12), C4 (n=17), C5 (n=10), C6 (n=17), C7 (n=8), C8 (n=17), R^2 = 99.85 %. The data of each sample are displaced by the abscissa to avoid overlapping of points and fitting curves

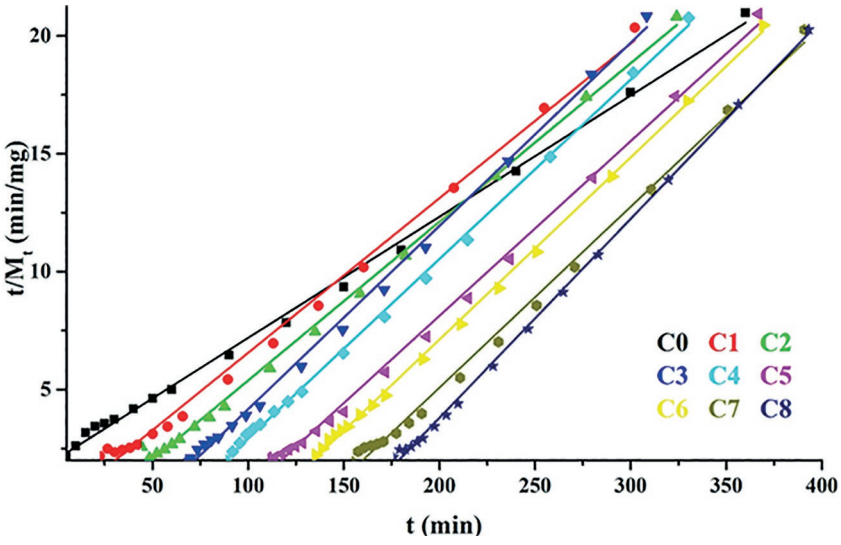

Fig. S5 - Fitting of experimental data to **Eq. 8** (pseudo 2nd order). N = 16 for all the samples, R^2 = 99.63 %. The data of each sample are displaced by the abscissa to avoid overlapping of points and fitting curves.

REFERENCES

1. S. Merino, C. Martín, K. Kostarelos, M. Prato, E. Vázquez, Nanocomposite hydrogels: 3D polymer–nanoparticle synergies for on-demand drug delivery, *ACS Nano* **9** (2015) 4686–4697
2. L.A. Sharpe, A.M. Daily, S.D. Horava, N.A. Peppas, Therapeutic applications of hydrogels in oral drug delivery, *Expet Opin. Drug Deliv*. **11** (2014) 901–915.
3. Y. Campos, G. Fuentes, J.A. Delgado, A. Almirall, Preparation and characterization of hydrophilic composites AA/EPMA loaded with hydroxyapatite, *J. Biomed. Mater. Res.* **101A** (2013) 3607–3615
4. A.N. Zelikin, C. Ehrhardt, A.M. Healy, Materials and methods for delivery of biological drugs, *Nat. Chem.* **8** (2016) 997
5. H.S. Yoo, T.G. Kim, T.G. Park, Surface-functionalized electrospun nanofibers for tissue engineering and drug delivery, *Adv. Drug Deliv. Rev*. **61** (2009) 1033–1042
6. W.J.E.M. Habraken, J.G.C. Wolke, J.A. Jansen, Ceramic composites as matrices and scaffolds for drug delivery in tissue engineering, *Adv. Drug Deliv. Rev.* **59** (2007) 234–248
7. V. Mouriño, A.R. Boccaccini, Bone tissue engineering therapeutics: controlled drug delivery in three-dimensional scaffolds, *J. R. Soc. Interface* **7** (2010) 209–227
8. A.C. McLaren, Alternative materials to acrylic bone cement for delivery of depot antibiotics in orthopaedic infections, *Clin. Orthop. Relat. Res.* **427** (2004) 101–106
9. A.K. Bajpai, R. Singh, Preparation and characterization of hydroxyapatite impregnated semi-interpenetrating polymer networks (IPNs) of polyvinyl alcohol and poly(acrylamide-co-acrylic acid), *J. Macromol. Sci. Pure Appl. Chem.* **A41** (2004) 1135–1159
10. M.L. Gómez, A. Gallastegui, M.B. Spesia, H.A. Montejano, R.J. Williams, C.M. Previtali, Synthesis of poly(HEMA-co-AAm) hydrogels by visible-light photopolymerization of aqueous solutions containing aspirin or ibuprofen: analysis of the initiation mechanism and the drug release, *Polym. Adv. Technol.* **28** (2017) 435–442
11. B. Singh, R. Bala, Radiation formation of psyllium cross-linked poly(hydroxyethylmethacryla-te)-co-poly(acrylamide) based sterile hydrogels for drug delivery applications, *Polym. Sci.* **59** (2017) 363–375
12. T. Demirtas, A.G. Karakecili, M. Gumusderelioglu, Hydroxyapatite containing superporous hydrogel composites: synthesis and in-vitro characterization, *J. Mater. Sci. Mater. Med.* **19** (2008) 729–735
13. N. Pramanik, S. Mohapatra, P. Pramanik, P. Bhargava, Processing and properties of nano-hydroxyapatite(n-HAp)/poly(ethylene-Co-acrylic acid)(EAA) composite using a phosphonic acid coupling agent for orthopedic applications, *J. Am. Ceram. Soc.* **90** (2007) 369–375
14. G.S. Sailaja, P. Ramesh, H.K. Varma, Ultrastructural evaluation of in vitro mineralized calcium phosphate phase on surface phosphorylated poly(hydroxy ethyl methacrylate-co-methyl methacrylate), *J. Mater. Sci. Mater. Med.* **21** (2010) 1183–1193
15. K.P. Burnham, D.A. Anderson, Multimodel inference: understanding AIC and BIC in model selection, *Socio. Methods Res.* **33** (2004) 261–304
16. K.P. Burnham, D.R. Anderson, K.P. Huyvaert, AIC model selection and multimodel inference in behavioral ecology: some background, observations, and comparisons, *Behav. Ecol. Sociobiol.* **65** (2010) 23–35

17. G. Fuentes, E. Peón, Y. Campos, N. López, C.X. Resende, G.D.A. Soares, Application of new statistical approach to study drug release from OCP coating on titanium sheets, *Key Eng. Mater*. **396–398** (2009) 511–514.

18. G. Fuentes, O. Valdés, D. Zaldívar, L. Agüero, I. Katime, A new statistical point of view to choose a better linear model for reactivity and microstructure analysis in HEMA/furfuryl acrylate copolymerization process, Adv. Mat. Lett. 4 (2013) 534–542

19. H. Akaike, A new look at the statistical model identification, *IEEE Trans. Automat. Contr.* **19** (1974) 716–723.

20. G. Schwarz, Estimating the dimension of a model, Ann. Stat. 6 (1978) 461–464

21. G. Fuentes, M. González, G. Pérez, J.A. Delgado, E. Peón, M.L. Rojas, J.D. Casquero, P. Miranda, Influence of the composition on setting time and porosity in hydroxyapatite cements with alginate and chitosan, *Lat. Am. Appl. Res.* **35** (2005) 289–294.

22. P.L. Ritger, N.A. Peppas, A simple equation for description of solute release. I. Fickian and non-Fickian release from non-swellable devices in the form of slabs, spheres, cylinders or discs, *J. Contr. Release* **5** (1987) 23–36.

23. T. Higuchi, Rate of release of medicaments from ointment bases containing drugs in suspension, *J. Pharmacol. Sci*. **50** (1961) 874–875.

24. J.L. Escobar, D. Zaldivar, L. Agüero, S. Fernández, I. Katime, Liberación de cefazolina sódica a partir de hidrogeles de copolímeros de poli(acrilamida-co-ácido metacrílico), *Revista Iberoamericana de Polímeros* **1** (2003) 1–10.

25. R.W. Korsmeyer, R. Gurny, E. Doelker, P. Buri, N.A. Peppas, Mechanisms of solute release from porous hydrophilic polymers, *Int. J. Pharm*. **15** (1983) 25–35

26. R. Korsmeyer, S.R. Lustig, N.A. Peppas, Solute and penetrant diffusion in swellable polymers. I. Mathematical modeling, *J. Polym. Sci., Polym. Phys. Ed.* **24** (1986) 395–408.

27. W. Lindner, B. Lippold, Drug release from hydrocolloid embeddings with high or low susceptibility to hydrodynamic stress, Pharmaceut. Res. 12 (1995) 1781–1785,

28. N.A. Peppas, J.J. Sahlin, A simple equation for the description of solute release. III. Coupling of diffusion and relaxation, *Int. J. Pharm.* **57** (1989) 169–172.

29. E. Vallés, D. Durando, I. Katime, E. Mendizábal, J.E. Puig, Equilibrium swelling and mechanical properties of hydrogels of acrylamide and itaconic acid or its esters, *Polym. Bull.* **44** (2000) 109–114

30. L. Serra, J. Doménech, N.A. Peppas, Drug transport mechanisms and release kinetics from molecularly designed poly(acrylic acid-g-ethylene glycol) hydrogels, *Biomaterials* **27** (2006) 5440–5451

31. W.J. Higuchi, Diffusional models useful in biopharmaceutics/drug release rate processes, *J. Pharmacol. Sci.* **56** (1967) 315–324.

32. J. Siepmann, N.A. Peppas, Higuchi equation Derivation, applications, use and misuse, *Int. J. Pharm.* **418** (2011) 6–12

33. K.P. Burnham, D.R. Anderson, Multimodel inference: understanding AIC and BIC in model selection, *Socio. Methods Res*. **33** (2004) 261–304

34. C. Elvira, J. Mano, J. San Román, R.L. Reis, Starch-based biodegradable hydrogels with potential biomedical applications as drug delivery systems, *Biomaterials* **23** (2002) 1955–1966

35. N.A. Peppas, Analysis of Fickian and non-Fickian drug release from polymers, *Pharm. Acta Helv*. **60** (1985) 110–111.

36. J. Siepmann, A. Göpferich, Mathematical modeling of bioerodible, polymeric drug delivery systems, *Adv. Drug Deliv. Rev.* **48** (2001) 229–247

37. P.L. Ritger, N.A. Peppas, A simple equation for description of solute release II. Fickian and anomalous release from swellable devices, *J. Contr. Release* **5** (1987) 37–42

38. S. Torrado, P. Frutos, G. Frutos, Gentamicin bone cements: characterisation and release (in vitro and in vivo assays), *Int. J. Pharm*. **217** (2001) 57–69

39. G.L. Mandell, W.A. Petri Jr., Fármacos antimicrobianos. Penicilinas, cefalosporinas y otros antibióticos ß-lactámicos, in: L.S. Goodman, A. Gillman (Eds.), Las bases farmacológicas de la terapeutica, ninth ed., McGraw Hill Interamericana, Ciudad México, 1996, pp. 1141–1171.